New Method To Reduce Oxygen Surface Inhibition by Photorelease of Boranes from Borane/Amine Complexes[#]

Andrei V. Fedorov,*,† Andrey A. Ermoshkin,§ Alex Mejiritski,‡ and Douglas C. Neckers*,§

Wright Photoscience Laboratory, Bowling Green State University, Bowling Green, Ohio 43403; Spectra Group Limited, Inc., Millbury, Ohio 43447; and Center for Photochemical Sciences, Bowling Green State University, Bowling Green, Ohio 43403

Received September 1, 2006; Revised Manuscript Received January 19, 2007

ABSTRACT: A new photochemical approach for free radical polymerization has been developed. The system releases trialkylborane from its complex with 4-(dimethylamino)pyridine upon irradiation. The presence of a free borane in the formulation, when it encounters oxygen, promotes radical polymerization. The system, when irradiated by an ergonomic 395 nm LED array, is able to efficiently overcome surface oxygen inhibition. The properties of the resulting photopolymer surfaces either matched or exceeded those of controls polymerized under N_2 atmosphere or with high-intensity light source. Results of experimental and computational studies probing the mechanism of borane photorelease are also discussed.

Introduction

Photopolymerization is widely utilized for converting vinyl monomers to polymers,[1] the applications of which have grown significantly over the past few decades. The principal advantages of using light to produce photopolymers include low cost, absence of volatile organic compounds, reduced energy consumption, rapid processing times, and ambient temperature requirements. Since light can be turned on or off, photopolymerizations can be started and stopped on demand. Photoprocesses can be used in imaging which is another advantage. There are also limitations. Polymerizable surfaces of a complex shape might not be entirely accessible for light, cationic polymerization is moisture sensitive and free radical polymerization is inhibited by oxygen.

The latter results from reaction of the initiating carbon-centered radicals ($R^•$) with oxygen (O_2) producing unreactive peroxy radicals ($R-O-O^•$).[1,2] In addition, the triplet ground state of oxygen readily quenches the excited triplet state of most photoinitiators. Oxygen inhibition, thus, competes with the reactive pathways responsible for the initiation of polymerization.[2,3] The inhibitory effect is especially pronounced on the surface of a to-be-polymerized substrate where there is an unlimited supply of oxygen present. As a result, if not properly dealt with, a surface is produced that is underpolymerized compared to the bulk of the polymer.

Known methods that counter oxygen surface inhibition[3] may include providing an inert atmosphere, the application of light of high irradiance,[4] and/or the creation of a physical barrier that restricts O_2 access.[5] Another strategy utilizes monomers that are less prone to oxygen inhibition like ethylene or propylene glycol and/or thioether acrylates.[3] The introduction of additives capable of rapid consumption of O_2 such as amines or *N*-vinylamides,[6] phosphites or phosphines,[7] and thiols[8,9] is another method. In addition, an interesting photochemical method to counter the effect of oxygen utilizes properties of excited porphyrins.[10] Despite significant effort and a variety of approaches, all methods that counter oxygen surface inhibition in radical polymerization have shortcomings and provide only partial or expensive solutions.

Organoboranes initiate radical polymerization in a reaction that requires molecular oxygen[11] though they react vigorously with oxygen, making it difficult to control their stability in formulations. Complexing boranes with amines or ethers drastically reduces the reactivity of the borane.[12] Amine complexes are effectively Lewis acid/base salts from which borane may be released by an agent capable of forming a stronger complex with the amine such as acid, aldehyde, or isocyanate. This release is the basis for several commercial two-part adhesive compositions.[13] The novel approach described herein photoreleases borane from its complex with an amine.

Experimental Section

Materials. Trimethylolpropane triacrylate (TMPTA) [Sartomer] was used as received. 4-(*N*,*N*-Dimethylamino)pyridine (4DMAP, 96% pure), *N*,*N*-dimethylaniline (DMA, 95% pure), 2,6-diisopropyl-*N*,*N*-dimethylaniline (DIDMA, 95% pure), 4-methoxypyridine (97% pure), 4-*tert*-butylpyridine (99% pure), triethylborane (TEB, >95% pure), and tributylborane (98% pure) were obtained from Aldrich and used without further purification. Benzophenone (99% pure, Aldrich) was recrystallized from toluene/hexanes prior to use. Pyridine (99% pure, Acros) was distilled from KOH prior to use. 2-Ethylhexyl-4-(dimethylamino)benzoate (ODAB; First Chemical Corp., 98% pure) and isopropylthioxanthone (ITX; New Sun Chemical Co. Ltd., 98% pure) were used as received. Benzene (HPLC grade, >99.9% pure) was purchased from Aldrich. THF (obtained from EMD) was refluxed over Na/K alloy for 4 h and distilled in an Ar atmosphere to obtain oxygen-free solvent.

General Procedures. ^{1}H NMR spectra were recorded using a 300 MHz Bruker Avance 300 nuclear magnetic resonance spectrometer. ^{11}B NMR spectra were recorded using 400 MHz Varian Unity Plus system. The resonance frequency for ^{11}B was 128 MHz. FTIR spectra were measured using a Shimadzu 8400S spectrometer. Sample irradiation was carried out using either an array of 395 nm LEDs[14] purchased from Clearstone Inc. equipped with CF1000 power supply or with a mercury lamp system from Fusion Inc. (model P300 equipped with the 300 W/in. H bulb).

* Corresponding authors. E-mail: avfedor@bgnet.bgsu.edu; neckers@photo.bgsu.edu.
† Wright Photoscience Laboratory, Bowling Green State University.
‡ Spectra Group Limited, Inc.
§ Center for Photochemical Sciences, Bowling Green State University.
[#] Contribution No. 611 from the Center for Photochemical Sciences.

10.1021/ma062025+ CCC: $37.00
Published on Web 04/18/2007

Table 1. Comparison of the Photopolymerization Efficiency of Borane Photorelease System to Various Controls

property of the polymer	irr time, min[b]	Et_3B·4DMAP 8.5%(3%)$_{mass}$ ITX 3.5%$_{mass}$ 3:1 mol[c] (1:1 mol)[d]	4DMAP 4.9%(3%)$_{mass}$ ITX 3.5%$_{mass}$ 3:1 mol[c] (1:1 mol)[d]	ODAB 11%(3.6%)$_{mass}$ ITX 3.5%$_{mass}$ 3:1 mol[c] (1:1 mol)[d]	ODAB 11%$_{mass}$ ITX 3.5%$_{mass}$ 3:1 mol[c] under N_2	ODAB 11%$_{mass}$ ITX 3.5%$_{mass}$ 3:1 mol[c] H-bulb[e]
surface hardness[a]	1	**14.4** (3)	**9.3** (0)	**6.8** (1)	**8**	
	3	**20.5** (9.5)	**11.6** (0)	**8.6** (4.3)	**9**	**11**
	5	**18.6** (13.7)	**12.1** (0.2)	**9.4** (6.4)	**11**	
surface %DB (ATR)	1	**82.6** (61.5)	**65.9** (42.1)	**75.8** (41.6)	**83.7**	
	3	**82.2** (70.8)	**67.9** (49.6)	**78.8** (51.5)	**85.6**	**95.5**
	5	**83.7** (75.4)	**69.4** (50.7)	**80.1** (53.9)	**85.0**	
through %DB (near IR)	1	**76.3** (67.9)	**74.0** (55.8)	**67.5** (64.9)	**68.2**	
	3	**79.8** (71.8)	**76.9** (60.6)	**71.7** (67.0)	**69.0**	**75.3**
	5	**79.5** (73.6)	**80.9** (60.6)	**74.0** (67.0)	**70.4**	

[a] Measured relative to glass surface hardness of 41. [b] Irradiated by a 395 nm LED light source except for the data from the last column. [c] Numbers in bold correspond to a 3:1 synergist/ITX ratio. [d] Numbers in parentheses correspond to a 1:1 synergist/ITX ratio. [e] Irradiated by a triple pass under Fusion H-bulb system.

Synthesis of Triethylborane/4-(Dimethylamino)pyridine Complex. *Precautions were taken to keep all reagents and the reaction mixture under an atmosphere of dry argon since triethylborane was pyrophoric*.

4-(Dimethylamino)pyridine (4.16 g, 34.08 mmol) was placed in a 100 mL round-bottom flask. The flask was filled with dry argon, and then 30 mL of absolute, oxygen-free THF was added. Triethylborane (3.34 g, 34.08 mmol) and absolute, oxygen-free THF (7 mL) were mixed in a syringe and transferred completely to the reaction flask by dropwise addition to a stirred solution of 4-(dimethylamino)pyridine cooled in an ice−water bath. The resulting mixture was stirred for 15 min followed by solvent removal by a rotary evaporation. The system was purged with dry argon prior to disconnecting the flask. The white crystalline product obtained was dried at 20 °C under vacuum for 2 h followed by purging the flask with dry argon. The amount of product obtained was 7.45 g (99.2% yield). ^{1}H NMR (300 MHz, $CDCl_3$), δ, ppm: 8.05 (d, J = 7.2 Hz, 2H, 2-Ar*H*, + 6-Ar*H*), 6.53 (d, J = 7.2 Hz, 2H, 3-Ar*H*, + 5-Ar*H*), 3.09 (s, 6H, CH_3), 0.59 (t, J = 7.8 Hz, 9H, BCH_2-CH_3), 0.35 (q, J = 7.8 Hz, 6H, $B-CH_2$). ^{13}C NMR (75 MHz, $CDCl_3$), δ, ppm: 154.39 (1C, *C4*-Py), 144.48 (2C, *C2*-Py + *C6*-Py), 106.04 (2C, *C3*-Py + *C5*-Py), 39.22 (2C, $N(CH_3)_2$), 14.95 (m, 3C, CH_2-B), 9.69 (3C, BCH_2-CH_3). ^{11}B NMR (128 MHz, $CDCl_3$), δ ($Et_2O{\cdot}BF_3$, ppm): −0.11.

Synthesis of Triethylborane/Pyridine and Triethylborane/Substituted Pyridine Complexes. The complexes of triethylborane with pyridine, 4-methoxypyridine, and 4-*tert*-butylpyridine were synthesized using methodology similar to the one described above.

Py/Et$_3$B. ^{1}H NMR (300 MHz, $CDCl_3$), δ, ppm: 8.55 (m, 2H, 2-Py*H* + 6-Py*H*), 7.89 (m, 1H, 4-Py*H*), 7.51 (m, 2H, 3-Py*H* + 5-Py*H*), 0.59 (t, J = 7.8 Hz, 9H, BCH_2-CH_3), 0.45 (q, J = 7.8 Hz, 6H, $B-CH_2$). ^{13}C NMR (75 MHz, $CDCl_3$), δ, ppm: 145.64 (2C, *C2*-Py + *C6*-Py), 138.27 (1C, *C4*-Py), 124.68 (2C, *C3*-Py + *C5*-Py), 15.39 (m, 3C, CH_2-B), 9.49 (3C, BCH_2-CH_3). ^{11}B NMR (128 MHz, $CDCl_3$), δ ($Et_2O{\cdot}BF_3$, ppm): 2.56.

4-MeO−Py/Et$_3$B. ^{1}H NMR (300 MHz, $CDCl_3$), δ, ppm: 8.34 (m, 2H, 2-Py*H* + 6-Py*H*), 6.94 (m, 2H, 3-Py*H* + 5-Py*H*), 3.94 (s, 3H, CH_3O), 0.58 (t, J = 7.8 Hz, 9H, BCH_2-CH_3), 0.39 (q, J = 7.8 Hz, 6H, $B-CH_2$). ^{13}C NMR (75 MHz, $CDCl_3$), δ, ppm: 166.71 (1C, *C4*-Py), 146.83 (2C, *C2*-Py + *C6*-Py), 110.35 (2C, *C3*-Py + *C5*-Py), 55.90 (1C, CH_3O), 14.99 (m, 3C, CH_2-B), 9.54 (3C, BCH_2-CH_3). ^{11}B NMR (128 MHz, $CDCl_3$), δ ($Et_2O{\cdot}BF_3$, ppm): 1.51.

4-tert-Bu-Py/Et$_3$B. ^{1}H NMR (300 MHz, $CDCl_3$), δ, ppm: 8.42 (m, 2H, 2-Py*H* + 6-Py*H*), 7.46 (m, 2H, 3-Py*H* + 5-Py*H*), 1.36 (s, 9H, $(CH_3)_3$C), 0.59 (t, J = 7.8 Hz, 9H, BCH_2-CH_3), 0.43 (q, J = 7.8 Hz, 6H, $B-CH_2$). ^{13}C NMR (75 MHz, $CDCl_3$), δ, ppm: 163.16 (1C, *C4*-Py), 145.06 (2C, *C2*-Py + *C6*-Py), 121.67 (2C, *C3*-Py + *C5*-Py), 35.17 (1C, $(CH_3)C$), 30.29 (3C, $(CH_3)C$), 15.02 (m, 3C, CH_2-B), 9.56 (3C, BCH_2-CH_3). ^{11}B NMR (128 MHz, $CDCl_3$), δ ($Et_2O{\cdot}BF_3$, ppm): 1.80.

Photopolymerization Experiments. Photopolymerizable formulations (5 g) were prepared by dissolving the designated reagents (see Table 1) in TMPTA. The formulations were prepared and handled in the dark until use. A 270 μm layer of formulation was deposited on a 2 in. by 3 in. microscope glass slide to cover an area of ca. 1.5 in. by 2.5 in. This was followed by exposure to the output of a 395 nm LED light source (10 cm distance; dose per minute of exposure: 272 mJ cm^{-2}) for a designated time. Choice of the LED-based light source was dictated by its low electrical power consumption and very efficient absorption of its narrow emission by the ITX photoinitiator.[14] The degree of double-bond conversion and extent of surface cure obtained in the polymerized layers were measured. The system under investigation (ITX + 4DMAP·BEt_3 complex) was judged against several controls including ITX + free 4DMAP as well as the commonly used combination of ITX + ODAB. Additional controls included irradiating under an atmosphere of N_2 and exposure to high-intensity industrial mercury vapor light source (Fusion System, H-bulb, dose for a single pass with 10 ft min^{-1} belt speed: 1420 mJ cm^{-2}).

Measurement of Double-Bond Conversion. The degree of a double-bond conversion (%DB) was measured as described previously by comparing changes in the near-IR before and after irradiation.[15,16] In the 5000−6500 cm^{-1} region, the first overtones of the olefinic and aliphatic CH stretches are separated, in contrast to the overlapping transitions of the fundamental (2900−3000 cm^{-1}) region. This permits a separate evaluation of the CH olefinic and CH aliphatic regions. As double bond converts during the polymerization, the CH olefinic signal decreases. The %DB could be calculated by comparing the CH olefinic signals for polymerized and unpolymerized samples. Since the overtone signals are weaker, relatively thick films that yield saturated mid-IR spectra could be analyzed.

A glass slide containing the polymer film was inserted into the cell holder to measure the near IR spectrum in the range from 5000 to 6500 cm^{-1} with 30 scans and 2 cm^{-1} resolution. Spectra were collected in the transmission mode. The ratios of the area between the peaks in the olefinic (6100−6300 cm^{-1}) and aliphatic (5500−6100 cm^{-1}) regions of the first overtone of the CH stretch were measured (I_t) and compared to those from the unexposed sample (I_0). Double-bond conversion was calculated using the following equations:

$$I_0 = A^0_{ol}/A^0_{al} \qquad I_t = A^t_{ol}/A^t_{al} \qquad \%DB = \frac{I_0 - I_t}{I_0} \times 100\%$$

where A_{ol} is the area under the peak in the olefinic CH region and A_{al} is the area under the peaks in the aliphatic CH region. To obtain I_0, the near-IR spectrum was measured by placing an unexposed liquid sample in an IR cell equipped with rectangular CaF_2 windows and 1 mm Teflon spacer. Photopolymerization profiles were obtained point-by-point by measuring the final %DB in the near-IR for samples irradiated for designated periods of time.

Surface Cure Measurements. Two properties of the polymerized surfaces were evaluated: surface hardness and %DB at the surface. Surface hardness is directly related to the efficiency of

Scheme 1

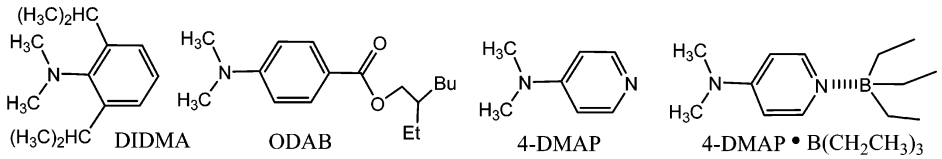

Scheme 2

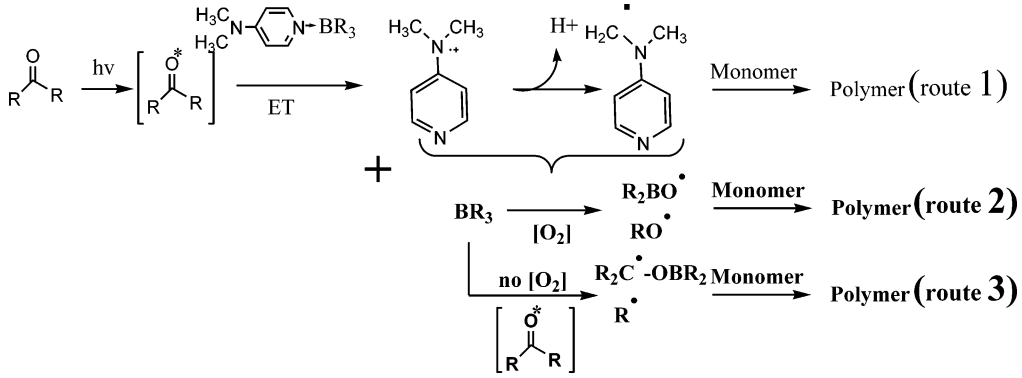

polymerization on the surface and can be measured quantitatively (ASTM D2134) using a Gardner Sward Hardness Rocker (model GSI). Rocker cycles are electronically determined and registered on a display which evaluates surface hardness relative to glass which registers a value of 41. The surface tested was kept horizontal, and measurements were conducted in a box eliminating the influence of air flow. The values reported represent an average of at least five measurements.

The %DB at the surface was measured by a ThermoNicolet IR200 FTIR spectrometer equipped with a diamond attenuated total reflectance (ATR) attachment. The following acquisition parameters were used: 700−4000 cm^{-1} spectral range; 30 scans; 2 cm^{-1} resolution. %DB was monitored by the decrease in the area of the acrylic wag peak at 809 cm^{-1} internally referenced to the area under either the carbonyl or CH mid-IR peaks.[15]

Laser Flash Photolysis. The difference in reactivity of benzophenone triplet state with the complex of triethylborane and 4-(dimethylamino)pyridine and that of uncomplexed 4-(dimethylamino)pyridine was evaluated using laser flash photolysis. Control experiments were conducted where benzophenone triplet state was quenched by aromatic tertiary amines as well as BEt_3 complexes with several 4-substituted pyridines. In addition, the reactivity of uncomplexed borane with benzophenone triplet was examined. All experiments were conducted using the laser flash photolysis setup described in detail previously.[17] Frequency-tripled (355 nm) pulses from a Q-switched Nd:YAG laser operating at the 10 Hz repetition rate were used for excitation. The pulse energy was 10 mJ, and the pulse duration was ca. 7 ns.

The samples tested consisted of an appropriate quencher in concentrations of 0.5, 1, 2, 3, 5, 8, and 10 mM obtained by dilution of a 20 mM solution and a 6.75 mM solution of benzophenone in benzene. All solutions were degassed prior to measurement by purging with Ar for 20 min. For oxygen-sensitive compounds, all manipulations and transfers were conducted under an Ar atmosphere.

Calculations. All calculations were performed using Gaussian 03 for Windows.[18] Optimization of the ground state geometries and vibrational frequencies (scaled by 0.96) were made at the density functional (DFT B3LYP/6-31++G(d,p)) level of theory. No imaginary frequencies were observed for all optimized structures indicating the true minima. The complexation energy was calculated as a difference between the energy of the complex and energies of the corresponding complex constituents. Complexation energy was corrected for zero-point vibrational energy contributions but was not corrected for basis set superposition errors.

Results and Discussion

Aromatic ketone photoiniators generate radicals when they react with tertiary amines by an initial electron transfer caused by the excited carbonyl triplet state (^{3}[⟩C═O]*). This produces an ammonium radical cation that subsequently deprotonates. Alkyl tertiary amines ($(R-CH_2)_2NR'$) are excellent electron donors.[1] The $^{\bullet}$CRH−N radicals eventually formed are known to reduce oxygen surface inhibition.[3] Dimethylaniline (DMA, IP = 7.37 eV[19a]) derivatives, 2,6-diisopropyl-*N*,*N*-dimethylaniline (DIDMA, IP = 7.85 eV[19b]), and 2-ethylhexyl-4-(dimethylamino)benzoate (ODAB, no IP data available) are often used in photopolymerization (Scheme 1).

Bifunctional 4-(dimethylamino)pyridine (4DMAP, IP = 7.82 eV[19c]) is the core of the system investigated in this work. While the dimethylamino functionality may interact with the aromatic carbonyl compound triplet state, the pyridyl nitrogen is the complexation site of the trialkylborane. Donation of an electron to ^{3}[⟩C═O]* is followed by formation of $^{\bullet}CH_2N$ radical which alters the overall electronic composition. This disrupts the complexation between boron and nitrogen. Thus, photoexcitation of the carbonyl compound in the presence of the complex of borane with an amine not only enables the generation of active radicals but also opens a second route to initiate radical polymerization by liberating borane from its complex (Scheme 2). This latter route is promoted by the presence oxygen and is expected to contribute most significantly at the surface. Upon consumption of oxygen within the formulation volume, a third route to polymerization becomes available owing to direct interaction of a free borane with excited benzophenone (vide infra). In addition, the presence of a free borane in the formulation provides another advantage—it may improve the adhesion to substrates including low-energy surfaces.[11,13]

We have compared our experimental system to industrially accepted packages containing isopropylthioxanthone (ITX) photoinitiator and ODAB synergist as well as to polymerizations conducted under an atmosphere of N_2 or caused by using high-intensity H-bulb light source from Fusion Inc. (Table 1). We have evaluated the %DB for the bulk polymer as well as the surface properties of the resulting polymer.

The results of near-IR double-bond conversion measurements (Figure 1, Table 1) clearly demonstrate that the complex of 4DMAP with $B(CH_2CH_3)_3$ performs well with ITX photoini-

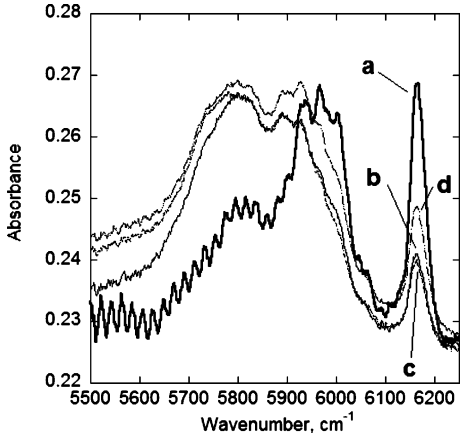

Figure 1. Near-IR spectra (a) before 395 nm irradiation and after 5 min irradiation of trimethylolpropane triacrylate and isopropylthioxanthone photoinitiator (0.68 mmol) containing (b) 2.08 mmol of 2-ethylhexyl-*p*-(dimethylamino)benzoate, (c) 0.68 mmol of 4-(dimethylamino)pyridine/BEt_3, and (d) 0.68 mmol of 4-(dimethylamino)-pyridine.

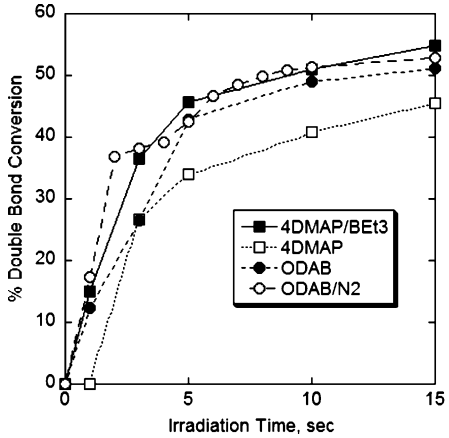

Figure 2. Kinetics of photopolymerization of trimethylolpropane triacrylate containing isopropylthioxanthone and complex of triethylborane with 4-(dimethylamino)pyridine (black squares), uncomplexed 4-(dimethylamino)pyridine (hollow squares), ODAB (black circles), and ODAB polymerized under N_2 (hollow circles).

tiator, giving an overall %DB (79.5%) comparable to that obtained for the industrially used ODAB (74.0%). Free, uncomplexed 4DMAP also yields good %DB (80.9%).

Each of the experiments (Table 1), except for that in the free 4DMAP in 1:1 molar ratio, resulted in tack-free surfaces. The surface hardness of resulting polymers provides important information about the relative efficiency of the formulations in preventing oxygen inhibition of polymerization at the surface. A surface hardness of 18.6 of our experimental system (column 3) exceeds that of the industrially utilized control (column 5) by a factor of 2 after 5 min of irradiation. Even when ITX/ODAB formulation is irradiated under N_2 (column 6) or with high-intensity H-bulb source (column 7), the experimental system yielded a surface hardness that is 1.7 times higher.

Values of %DB at the surface (Table 1, row 2) support the observations obtained from the surface hardness measurements. The experimental system outperforms controls containing either 4DMAP or ODAB when ITX/synergist ratios are similar. Irradiation by high-power H-bulb yields the highest surface %DB, as expected.

The polymerization occurs faster for the formulation containing Et_3B·4DMAP than for controls containing uncomplexed 4DMAP and ODAB synergists (Figure 2). Moreover, an initial polymerization rate of Et_3B·4DMAP is matched well with that of the ODAB/N_2 control where the blanket of nitrogen prevents surface inhibition by oxygen. The formulation containing Et_3B·4DMAP shows no induction period such as that clearly seen for the control containing only 4DMAP. We attribute this enhanced performance to the additional polymerization routes enabled by the trialkylborane released.

Three pathways are possible for the release of borane from the complex following electron transfer. The excited carbonyl moiety may interact with the dimethylamino functionality of 4DMAP and trigger the release through significant change of an electron density of this molecule owing to electron/proton transfer. It may also directly compete with a complexed borane at the pyridyl nitrogen site. Another possibility may include an electron transfer to excited carbonyl moiety from a complexed borane, which inherits some electron density upon complexation.

In order to probe the second and third pathways, we have examined complexes of triethylborane with other diamines where two nitrogen sites are not linked via π-system like in 4DMAP. For both hexamethylenediamine and 1,2-diaminopropane (Table 2), we did not see such a reduction of the polymerization inhibition at the surface as we have observed for 4DMAP complex. This suggests borane photorelease via communication between dimethylamino and pyridyl moieties.

Laser flash photolysis (LFP), in which benzophenone (Bp) was used to interact with the complex of borane with an amine and other model compounds, provides important information about the mechanism. The reaction between benzophenone triplet state and *N*,*N*-dimethylaniline (DMA) proceeds via fast electron transfer ($\sim 10^{11}$), resulting in formation of a contact ion pair.[20] The contact ion pair may next undergo separation as a result of thermal diffusion that has a rate constant of ca. 5×10^8 s^{-1}. The electron transfer is followed by a fast proton transfer ($k_{pt} = 1.3 \times 10^9$) in the ion pair formed.[20e] The overall result is a triplet radical pair (•BpH + •DMA). Bimolecular quenching rate constants in benzene (k_Q) of 6.00×10^9 and 2.74×10^9 M^{-1} s^{-1} for interaction of ^{3}Bp* with DMA and DIDMA, respectively, are close to the diffusion control limit, as expected (Table 3). The smaller quenching rate constant for DIDMA is stipulated by the steric hindrance from two isopropyl groups.

Table 2. Photopolymerization Efficiency for Systems Containing the Complexes of Triethylborane with Aliphatic Diamines

property of the polymer	irr time, min[b]	Et_3B·$(H_2N)_2(CH_2)_6$ (2.9% mass) ITX (3.5% mass) (1:1 mol)	Et_3B·$(H_2N)_2(CH_2)_6$ (1.5% mass) ITX (3.5% mass) (1:2 mol)	Et_3B·$CH_3CH(NH_2)$-CH_2NH_2 (2.4% mass) ITX (3.5% mass) (1:1 mol)	$CH_3CH(NH_2)CH_2NH_2$ (1% mass) ITX (3.5% mass) (1:1 mol)
surface hardness[a]	1	1	0	0	0
	3	3	0	0	0
	5	7.8	0	0	0
%DB conversion	1	59.6	53.8	52.8	44.3
	3	62.3	58.6	59.6	46.3
	5	66.0	60.7	63.3	50.1

[a] Measured relative to glass surface hardness of 41. [b] Irradiated by a 395 nm LED light source.

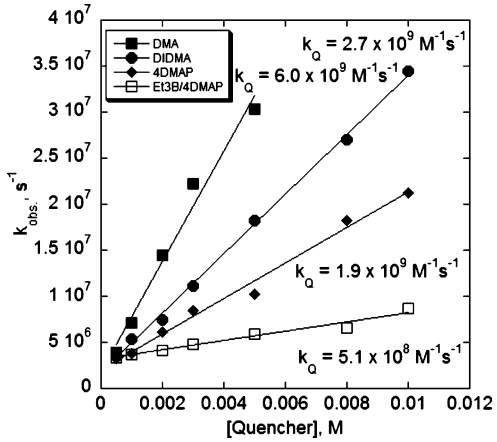

Figure 3. Dependence of the observed rate constant of benzophenone triplet decay on the concentration of dimethylaniline (black squares), 2,6-diisopropyl-*N*,*N*-dimethylaniline (black circles), 4-(dimethylamino)-pyridine (black diamonds), and 4-(dimethylamino)pyridine/triethylborane complex (hollow squares).

Table 3. Rate Constants of Bimolecular Quenching of Triplet Benzophenone by Various Systems

system	$k_Q \times 10^{-9}$, $M^{-1}\,s^{-1}$	system	$k_Q \times 10^{-9}$, $M^{-1}\,s^{-1}$
4DMAP/BEt_3	0.51 ± 0.04	DIDMA	2.74 ± 0.06
4DMAP	1.93 ± 0.09	pyridine	no reaction
DMA	6.00 ± 0.51		

Bimolecular ^{3}Bp* quenching by free 4DMAP yielded a rate constant of 1.93×10^9 M^{-1} s^{-1} (Figure 3 and Table 3), which is close to that of DIDMA. In this case, the reduction of reactivity relative to DMA may be explained by the electron-withdrawing effect of a pyridyl ring that makes 4DMAP a weaker donor of electron. However, quenching by the Et_3B·4DMAP complex is 12 times slower than that by DMA (k_Q = 5.10×10^8 M^{-1} s^{-1}). We assume that complexation with BEt_3 further depletes electron density from the dimethylamino moiety by engaging the lone electron pair of the pyridine nitrogen. This makes the complex a poorer donor of an electron/proton compared to free 4DMAP. The complex of borane with an amine reacts more slowly with the ^{3}[C═O]* moiety but initiates polymerization more efficiently. This is another confirmation that borane is released form the complex.

The lifetime of benzophenone triplet state did not change upon addition of up to 10 mM pyridine. This lack of reactivity eliminates the possibility of a photorelease pathway wherein the ^{3}[C═O]* moiety competes directly with the complexed borane at the pyridyl site.

The lifetime of a triplet benzophenone gradually decreases as the concentration of BEt_3 increases from 1 to 10 mM, indicating a direct reaction with borane (Figure 4). This is consistent with previous electron spin resonance (ESR) studies of trialkylborane quenching of the triplet state of aliphatic and aromatic ketones via homolytic bimolecular substitution (S_{H2}) at the boron atom.[21] The observed bimolecular quenching rates of $(2.30 \pm 0.10) \times 10^7$ for BEt_3 and $(2.32 \pm 0.22) \times 10^7$ for BBu_3 (Figure 4, inset) are in a good agreement with the previously reported data for BBu_3 ($k_Q = 4.6 \times 10^7$).[21b] This process is 1 order of magnitude slower than the quenching by dimethylamino moiety of the Et_3B·4DMAP complex. Therefore, the presence in solution of a free borane released from the complex should not affect the bimolecular quenching rate reported in Table 3.

Evidence from our LFP and previous ESR data on the reactivity of a free borane with triplet carbonyl moiety suggest the possibility of another route to radical polymerization (route 3 in Scheme 2). Free borane reacts with O_2 much faster than with the ^{3}[⟩C═O]* with the bimolecular rate constant for reaction with oxygen being controlled by the rate of O_2 diffusion in the medium.[22] However, within the bulk of the formulation, O_2 is completely consumed during the initial stage of polymerization without efficient routes to resupply it. In addition, it has been demonstrated that without oxygen or other additives present borane itself is inactive as initiator of radical polymerization.[23] Our experiments confirm this by detecting no difference in the NMR spectra before and after irradiation of solutions contanining Et_3B and ethyl acrylate. As polymerization proceeds, route 3 begins to contribute within the bulk of the polymer, assuming the presence of the photoexcitable carbonyl moiety in the formulation. Route 2 remains one of the dominant processes at the surface until complete consumption of BR_3.

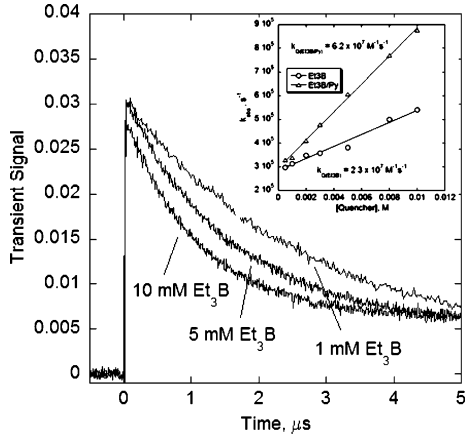

Figure 4. Decrease in the benzophenone triplet lifetime upon addition of 1, 5, and 10 mM triethylborane. Inset: dependence of the observed rate constants of benzophenone triplet decay on the concentration of triethylborane (hollow circles) and complex of triethylborane with pyridine (hollow triangles).

Table 4. Correlation between Reactivity of Various Boron Compounds and Their ^{1}H and ^{11}B NMR Chemical Shifts

system	$k_Q \times 10^{-7}$, $M^{-1}\,s^{-1}$	B-**CH_2**-R ^{1}H shift	**B**R_x ^{11}B shift
Et_3B	2.30 ± 0.10	1.19	86.7
Et_3B·pyridine	6.24 ± 0.14	0.45	2.56
Et_3B·(4MeO-Py)	5.40 ± 0.16	0.39	1.51
Et_3B·(4*t*-Bu-Py)	4.55 ± 0.27	0.43	1.80
Et_3B·4DMAP	51.2 ± 4.0	0.35	−0.11
$(Bu_4N)^+(Bu_3PhB)^-$	395 ± 7	0.26	−15.3

Complexation between BEt_3 and pyridine blocks an empty orbital of boron and the S_{H2} pathway is expected to be deactivated. Surprisingly, Et_3B·Py quenches ^{3}Bp* with a rate constant of $(6.24 \pm 0.14) \times 10^7$ M^{-1} s^{-1}, 3 times faster than that of the uncomplexed borane. Upon complexation, the boron atom gains some electron density from the lone pair of the pyridyl nitrogen. Depending on the strength of the complexation, the amount of negative charge on boron may differ. The relative electron density on the boron atom could be assessed on the basis of the shifts of the corresponding peaks in ^{1}H and ^{11}B NMR spectra (Table 4). Tetrasubstituted borate salts represent an extreme case where boron has −1 formal charge. These compounds are excellent electron donors with the electron-transfer rate constants approaching the diffusion-controlled limit.[24] Therefore, we suggest that electron transfer similar to that in borates occurs from the complexes of boranes with amines. This process is much slower because complexes of borane with an amine are weaker electron donors compared to tetrasubstituted borate salts.

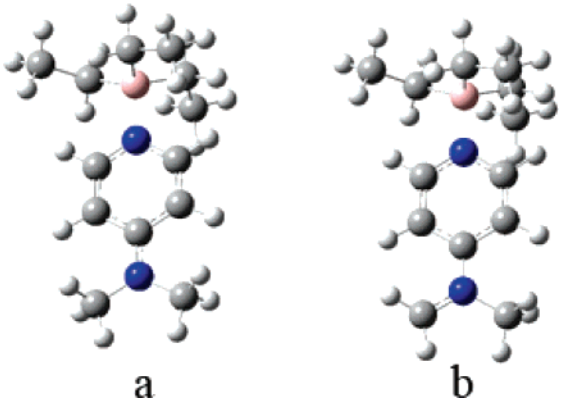

Figure 5. B3LYP 6-311G++(d,p) optimized geometries of a complex of BEt_3 with 4-(dimethylamino)pyridine (a: $E_{compl} = 6.65$ kcal/mol) and 4-(dimethylamino)pyridine radical (b: $E_{compl} = 5.83$ kcal/mol).

This hypothesis is supported by the results of the quenching experiments for complexes of Et_3B with 4-substituted pyridines. The triplet benzophenone quenching rate constants of $(5.40 \pm 0.16) \times 10^7$ and $(4.55 \pm 0.27) \times 10^7$ M^{-1} s^{-1} were obtained for Et_3B complexes with 4-methoxy- and 4-*tert*-butylpyridines, respectively. These data are close to the quenching rate observed for the complex of unsubstituted pyridine but 1 order of magnitude different from one observed for the complex with 4DMAP, despite the common electron-donating character of methoxy, *tert*-butoxy and dimethylamino moieties. In contrast to 4DMAP and similar to pyridine, uncomplexed 4-MeO-pyridine and 4-*tert*-butylpyridine did not quench benzophenone triplet in the 0.5−10 mM concentration interval. These observations confirm that (a) there exists an interaction between the ^{3}(Bp)* and Et_3B complexes with pyridine and substituted pyridines and (b) reactivity of Et_3B·4DMAP is determined by the NMe_2 moiety and not the pyridine/borane complexing site. Work is underway to further investigate the mechanism of the interaction between benzophenone triplet and complexes of borane with amines.

Optimized geometries of complexes of triethylborane with either 4DMAP ($E_{compl} = 6.65$ kcal/mol) or radical of 4DMAP ($E_{compl} = 5.83$ kcal/mol) formed as a result of H atom loss (an electron transfer followed by a proton transfer) from one of methyl moieties support the mechanism of borane photorelease from Et_3B·4DMAP (Figure 5). The complexation energy is calculated to decrease upon formation of radical from CH_3-N moiety by 0.82 kcal/mol. This indicates the weakening of complexation upon radical formation which creates the possibility of borane release from the complex.

In summary, we propose a new, efficient photochemical system that counters oxygen surface inhibition in radical photopolymerization. The approach utilizes chemistry of trialkylboranes released from their complexes with amines upon irradiation. The proposed systems perform well in combination with economical LED light sources and has a valuable potential for the coatings industry.

Acknowledgment. The authors acknowledge gratefully the Office of Naval Research for funding this project (Grant N00014-04-1-0406). Ohio Department of Development and Bowling Green State University are also acknowledged for funding this project through the Wright Photoscience Laboratory. The Ohio Laboratory for Kinetic Spectrometry is acknowledged for providing the LFP setup. We thank Prof. Michael Rodgers and Dr. Eugene Danilov for help in acquisition and interpretation of the time-resolved data.

References and Notes

(1) (a) Neckers, D. C.; Jager, W. *Chemistry & Technology of UV & EB Formulations for Coatings, Inks, and Paints*; Wiley/SITA Series in Surface Coatings Technology; John Wiley and Sons: Chichester, 1998; Vol. VII. (b) Fouassier, J. P. *Photoinitiation, Photopolymerization and Photocuring*; Verlag: New York, 1995.

(2) Krongauz, V. V. Diffusion in Polymer Matrix and Anisotropic Photopolymerization. In *Processes in Photoreactive Polymers*; Krongauz, V. V., Trifunac, A. D., Eds.; Chapman & Hall: New York, 1995; p 185.

(3) Hoyle, C. E. *Technical Conference Proceedings—UV & EB Technology Expo & Conference*; RadTech International North America: Chevy Chase, MD, 2004; pp 892−899.

(4) (a) Decker, C. *Polym. Int.* **1998**, *42*, 133−141. (b) Wight, F. R. *J. Polym. Sci., Polym. Lett. Ed.* **1978**, *16*, 121−127.

(5) (a) Selli, E.; Bellobono, I. R. Photopolymerization of Multifunctional Monomers: Kinetic Aspects. In *Radiation Curing in Polymer Science and Technology*; Fouassier, J. P., Rabek, J. F., Eds.; Elseiver Applied Science: London, 1993; Vol. III. (b) Decker, C.; Moussa, K. *Macromolecules* **1989**, *22*, 4455.

(6) Allen, N. S.; Johnson, M. A.; Oldring, P. K. T.; Salim, M. S. In *Chemistry & Technology of UV & EB Formulations for Coatings, Inks, and Paints*; Oldring, P. K. T., Ed.; SITA Technology: London, 1991; Vol. II.

(7) (a) Xiao, B.; Zhou, Y.; Li, S.; Luo, M.; Wang, X.; Zhao, P. *Radiat. Phys. Chem.* **2000**, *57*, 421−428. (b) Nakasuga, A. JP 01079213, 1989. (c) Schmitt, W.; Purrmann, R.; Jochum, P. DE 2811039, 1978.

(8) (a) Jacobine, A. T. In *Thiol-ene Photopolymers in Radiation Curing in Polymer Science and Technology*; Fouassier, J. P., Rabek, J. F., Eds.; Elseiver Science Publishers Ltd.: New York, 1993; Vol. III, pp 219−268. (b) Gush, D. P.; Ketley, A. D. *Mod. Paint. Coat.* **1978**, *68*, 61−72.

(9) (a) Krongauz, V. V.; Chawla, C. P.; Dupre, J. Oxygen and Radical Photopolymerization in Films. In *Photoinitiated Polymerization*; Belfield, K. D., Crivello, J. V., Eds.; *ACS Symp. Ser.* **2003**, *847*, 165. (b) Krongauz, V. V.; Chawla, C. P. Woodman, R. K. UV/EB, RadTech 2000: The Premier UV/EB Conference & Exhibition, Technical Conference Proceedings, Baltimore, MD, p 260. (c) Krongauz, V. V.; Chawla, C. P. *Polymer* **2003**, *44*, 3871.

(10) (a) Scranton, A. B.; Gou, L. Patent WO 2004062781, 2004. (b) Gou, L.; Coretsopolous, C. N.; Scranton, A. B. *J. Polym. Sci., Part A: Polym. Chem.* **2004**, *42*, 1285−1292.

(11) (a) Sonnenschein, M. F.; Webb, S. P.; Kastl, P. E.; Arriola, D. J.; Wendt, B. L.; Harrington, D. R.; Rondan, N. G. *Macromolecules* **2004**, *37*, 7974−7978. (b) Welch, F. J. *J. Polym. Sci.* **1962**, *61*, 243−252.

(12) For example see: Onak, T. *Organoborane Chemistry*; Academic Press: New York, 1957; pp 146−163 and references therein.

(13) (a) Webb, S. P.; Sonnenschein, M. F. US Pat. # 6,740,716. (b) Mottus et al. US. Pat. # 3,275,611. (c) Skoultchi et al. US Pat. # 5,106,928; 5,143,884; 5,286,821; 5,286,821; 5,310,835; 5,376,746. (d) Zharov et al. US Pat. # 5,539,070; 5,690,780; 5,691,065. (e) Pocius et al. US Pat. # 5,616,796; 5,621,143; 5,681,910; 5,686,544; 5,718,977; 5,795,-657.

(14) We have recently shown that irradiation by the latest commercially available powerful LED light sources provides photopolymerization results that are comparable to those obtained for conventionally used Hg lamp and Xe light sources. For more information see: Mejiritski, A.; Marino, T.; Martin, D.; Berger, D. J.; Fedorov, A. V.; Anyaogu, K. C.; Ermoshkin, A. A.; Neckers, D. C. Development of Corrosion Resistant Energy Curable Coatings. *RadTech Rep.* **2006**, *July/August*, 11−28.

(15) Decker, C.; Moussa, K. *Eur. Polym. J.* **1990**, *26*, 393.

(16) (a) Ermoshkin, A. A.; Neckers, D. C.; Fedorov, A. V. *Macromolecules* **2006**, *39*, 5669−5674. (b) Grinevich, O.; Snavely, D. L. *Chem. Phys. Lett.* **1999**, *304*, 202−206. (b) Grinevich, O.; Snavely, D. L. *Chem. Phys. Lett.* **1997**, *267*, 313−317.

(17) Merzlikine, A. G.; Voskresensky, S. V.; Fedorov, A. V.; Neckers, D. C. *Photochem. Photobiol. Sci.* **2004**, *3*, 892−897.

(18) Gaussian 03, Revision C.02: Frisch, M. J.; Trucks, G. W.; Schlegel, H. B.; Scuseria, G. E.; Robb, M. A.; Cheeseman, J. R.; Montgomery, Jr., J. A.; Vreven, T.; Kudin, K. N.; Burant, J. C.; Millam, J. M.; Iyengar, S. S.; Tomasi, J.; Barone, V.; Mennucci, B.; Cossi, M.; Scalmani, G.; Rega, N.; Petersson, G. A.; Nakatsuji, H.; Hada, M.; Ehara, M.; Toyota, K.; Fukuda, R.; Hasegawa, J.; Ishida, M.; Nakajima, T.; Honda, Y.; Kitao, O.; Nakai, H.; Klene, M.; Li, X.; Knox, J. E.; Hratchian, H. P.; Cross, J. B.; Bakken, V.; Adamo, C.; Jaramillo, J.; Gomperts, R.; Stratmann, R. E.; Yazyev, O.; Austin, A. J.; Cammi, R.; Pomelli, C.; Ochterski, J. W.; Ayala, P. Y.; Morokuma, K.; Voth, G. A.; Salvador, P.; Dannenberg, J. J.; Zakrzewski, V. G.; Dapprich, S.; Daniels, A. D.; Strain, M. C.; Farkas, O.; Malick, D. K.; Rabuck,

A. D.; Raghavachari, K.; Foresman, J. B.; Ortiz, J. V.; Cui, Q.; Baboul, A. G.; Clifford, S.; Cioslowski, J.; Stefanov, B. B.; Liu, G.; Liashenko, A.; Piskorz, P.; Komaromi, I.; Martin, R. L.; Fox, D. J.; Keith, T.; Al-Laham, M. A.; Peng, C. Y.; Nanayakkara, A.; Challacombe, M.; Gill, P. M. W.; Johnson, B.; Chen, W.; Wong, M. W.; Gonzalez, C.; Pople, J. A. Gaussian, Inc., Wallingford, CT, 2004.

(19) (a) Jatsuhashi, T.; Obayashi, T.; Tanaka, M.; Murakami, M.; Nakashima, N. *J. Phys. Chem. A* **2006**, *110*, 7763−7771. (b) Sibi, M. P.; Lichter, R. L. *J. Org. Chem.* **1977**, *42*, 2999−3004. (c) Ramsey, B. G.; Walker, F. A. *J. Am. Chem. Soc.* **1974**, *96*, 3314−3316.

(20) (a) Peters, K. S. *Adv. Photochem.* **2002**, *27*, 51−82. (b) Griller, D.; Howard, J. A.; Marriot, P. R.; Scaiano, J. C. *J. Am. Chem. Soc.* **1981**, *103*, 619−623. (c) Inbar, S.; Linschitz, H.; Cohen, S. G. *J. Am. Chem. Soc.* **1981**, *103*, 1048−1054. (d) Miyasaka, H.; Nagata, T.; Kiri, M.; Mataga, N. *J. Phys. Chem.* **1992**, *96*, 8060−8065. (e) Peters, K. S.; Kim, G. *J. Phys. Chem. A* **2001**, *105*, 4177−4181.

(21) (a) Davies, A. G.; Roberts, B. P.; Scaiano, J. C. *J. Chem. Soc. B* **1971**, 2171−2176. (b) Davies, A. G.; Scaiano, J. C. *J. Chem. Soc., Perkin Trans. 2* **1972**, 2234−2238.

(22) Davies, A. G.; Ingold, K. U.; Roberts, B. P.; Tudor, R. *J. Chem. Soc. B* **1971**, 698−712.

(23) Furukawa, J.; Tsuruta, T. *Bull. Inst. Chem. Res., Kyoto Univ.* **1960**, *38*, 319−351.

(24) (a) Schuster, G. B. *Pure Appl. Chem.* **1990**, *62*, 1565−1572. (b) Sarker, A. M.; Polykarpov, A. Y.; de Raaff, A. M.; Marino, T.; Neckers, D. C. L. *J. Polym. Sci., Part A: Polym. Chem.* **1996**, *34*, 2817−2824. (c) Hassoon, S.; Neckers, D. C. *J. Phys. Chem.* **1995**, *99*, 9416−9424. (d) Hassoon, S.; Sarker, A.; Rodgers, M. A. J.; Neckers, D. C. *J. Am. Chem. Soc.* **1995**, *117*, 11369−11370. (e) Polykarpov, A. Y.; Hassoon, S.; Neckers, D. C. *Macromolecules* **1996**, *29*, 8274−8276.

MA062025+